INDIAN JOURNAL OF SCIENCE AND TECHNOLOGY

RESEARCH ARTICLE

A Novel Image Denoising and Segmentation Using Machine Learning with SRM Strategy

Swaroopa H Narayan[1]*, **Basavaraj N Jagadale**[1], **Omar Abdullah Murshed Farhan Alnaggar**[1]

1 Department of PG Studies and Research in Electronics, Kuvempu University, Shankaraghatta, Shimoga, 577451, Karnataka, India

OPEN ACCESS

Received: 26-11-2021

Accepted: 24-03-2022

Published: 10.05.2022

Citation: Narayan SH, Jagadale BN, Murshed Farhan Alnaggar OA (2022) A Novel Image Denoising and Segmentation Using Machine Learning with SRM Strategy. Indian Journal of Science and Technology 15(17): 778-789. https://doi.org/10.17485/IJST/v15i17.2203

* **Corresponding author**.

swaroopaml@gmail.com

Funding: None

Competing Interests: None

Published By Indian Society for Education and Environment (iSee)

ISSN
Print: 0974-6846
Electronic: 0974-5645

Abstract

Objectives: In the last decade, artificial intelligence (AI) and machine learning (ML) have a significant impact on image analysis and segmentation. The most demanding aspect in digital image processing is efficient segmentation to extract the desired features or recognize the hidden patterns of the digital images, which are one of the major challenges. Even in existing segmentation techniques, due to under segmentation issues, particularly in remote or arial image analysis, necessary object features and residual details are not properly segmented. Therefore, the study presents a new method for image segmentation using machine learning, which addresses these limitations. **Methods:** This article presents a novel approach for arial image denoising and segmentation using unsupervised learning. The Discrete Wavelet Transform (DWT) is primarily used as a pre-processing tool, while edge details of the decomposed image are automatically preserved with the help of machine understanding. The use of a fast Non-Local (NL)-means filter provides a better visual effect for low-frequency image features, and the filtered image is partitioned into the number of clusters by Minimum-Spanning Tree **(**MST) clustering algorithm. Further, Statistical Region Merging (SRM) is used to eliminate the unwanted regions of the clustered image to give meaningful image details. Finally, the segmented image is projected at the wavelet restoration level. Here, the standard images are extracted from the SIPI database, and the system does not require training prototypes but works in an "unsupervised" way. **Findings:** The proposed system segment 1014 regions in the first phase and the segmented image features efficiently recognize the hidden patterns of the arial image (7.1.06). However, to track the required object features, statistical Region Merging (SRM) is utilized, a drastic variation in the merging process eliminates the annoying details and brings effective outcomes, which involves 29 essential features with retained residual details at level-2 decomposition and is compared with leading segmentation techniques. The denoising performance of the suggested study provides a 21.73 Peak Signal to Noise Ratio (PSNR) value in 17.96 elapsed time. The simulation results have proven to produce better segmentation and denoising with less iteration time. A qualitative evaluation through visual examination justifies the proposed study and is superior to some of the popular methods. **Novelty/Applications:** The utilization of wavelet transform to preserve edge features during segmentation is one of the key features of this method, and it significantly overcomes the under segmentation patterns. The combination of minimum-spanning tree clustering (MST) and statistical region merging (SRM) is the major strategic step in segmenting and detecting the essential object features of arial images.

Keywords: DWT; Fast NLmeans filter; Wavelet denoising; MST; SRM

1 Introduction

Remote or arial image analysis is one of the vital research area and plays a critical part in object detection and classification. Various image segmentation algorithms have been developed over the years, however, clustering algorithms have an essential role in the segmentation of digital images. Since unsupervised segmentation of images doesn't require prior knowledge, most of the clustering algorithms employ unsupervised segmentation. It recognizes the hidden patterns of the image to bring feasible outcomes[1–3]. Some clustering techniques try to separate regions based on similarity criteria, which look like the decomposition of the image into independent areas[4–9]. However, few machine learning algorithms don't provide a specific number of clusters during the partitioning process. Hence they generate as many clusters depending on the scaling factor of the image. Due to the extreme level of the clustering process, sometimes it is necessary to merge the unwanted or meaningless regions in an image, which helps to reduce the over-segmentation of the image[10–14]. Various region merging techniques were employed in the last few decades, to overcome the over/under segmentation patterns[15–17]. Nevertheless, based on the literature review, the combination of wavelet and watershed-based techniques in pre-processing phase is a superior technique in existing methods, the post-processing phase includes similarity based region merging, boundary-based merging, hierarchical merging, dynamic region merging and statistical region merging, etc, all these techniques arises from different predefined threshold criteria to merge required part of the image and the method provides better-segmented results only for standard images[18–21]. Image analysis and segmentation are essential needs in military and defense applications, which helps in recognizing the particular objects based on the requirements. The study mainly focused on Arial image denoising and segmentation. The existing methods provide better outcomes for standard image segmentation with the usage of discrete wavelet transform (DWT) at pre-processing level, and the region merging process is utilized at the post-processing level. But in the case of arial image, they lack consistency[22,23]. Therefore, the study suggests a new method, which is applicable for both normal as well as arial images. The simulation result of the conducted study is compared with some of the existing methods and is found to be significantly better in terms of denoising and segmentation. Visual inspection justifies the segmentation quality of the proposed method has effective outcome than existing methods, and it recognizes the object portion and provides meaningful image details at the wavelet restoration phase[24,25].

1.1 Discrete wavelet transforms (DWT

In DWT, the digital image is divided into four sub-images as, A (approximation coefficient or A1 band) contains most of the image information and D (detailed coefficients or H1, V1, D1 bands). However, detailed coefficients contain edge/texture details of the image along with residual noise. Here machine learning-based image denoising is employed, which selects the appropriate shrink filter to detailed coefficients based on some prior knowledge[(2–6)]. A1 band represents most of the low-frequency image features. Which is subjected to the pre-processing step and is further decomposed to level-2 based on requirement[(13–16)], as shown in Figure 1.

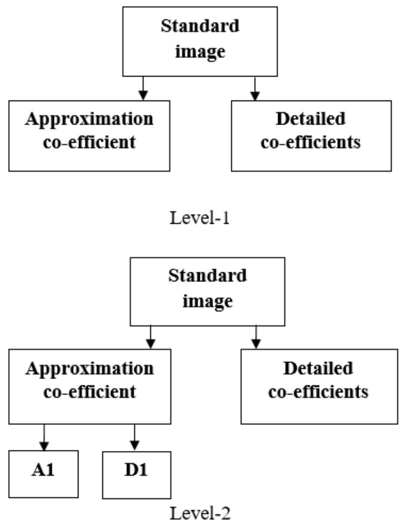

Fig 1. Schematicdiagram of Discrete wavelet Transform (DWT).

1.2 Fast NL-means filter

During the period of hypothetical design of the filter, the value of pixel 'i' is repaired,
where NL (v) (i) is given by

$$NL\ (v)\ (i) = \sum_{j \in i} w(i,j)\ v(j) \tag{1}$$

Where, v is the intensity function, and thus v(j) is the intensity at pixel j and w(i,j) the weight associated with v(j) in the reconstruction of pixel i. The unique description of the fast NL-means procedure reflects that every pixel can be connected. But virtually, the number of pixels taken into relation in the weighted mean is limited in a neighborhood. The likeness among i and j based on the correspondence of their native regions with mean Euclidean distance[(6–8)]. The general difficulty that arises in this process is the computational load with a neighborhood pixel grouping. Therefore, the purpose is to diminish the number of pixels taken into relation in the weighted mean and to evade recurring designs of the similar neighborhood[(9–12)].

$$w(i,j) = \begin{cases} \dfrac{1}{z(i)} e^{-\dfrac{\|v(N_i) - v(N_j)|_{2,a}^{2}}{h^2}} & \text{if } \mu_1 < \dfrac{\overline{v(N_i)}}{v(N_j)} < \mu^2 \text{ and } \sigma_2^1 < \dfrac{\mathrm{var}(v(N_i))}{\mathrm{var}(v(N_j))} < \sigma_2^2 \\ \text{othrewise.} & \end{cases} \tag{2}$$

where, z(i) is the normalization constant with $z(i) = \sum_j w(i,j)$ *and h* acts as a filtering parameter.
$v(N_i)$ *and* $v(N_j)v(N_i)$ *and* $v(N_j)$ is the similarity between the neighborhood pixel intensities.
"Distance between $v(N_i)$ *and* $v(N_j)$ is a standard norm $||1 - \|_a$, convolved by Gaussian-kernel of standard-deviation 'a', although measure of the distortion between pixel neighborhood intensities".

1.3 Minimum-spanning tree clustering

Clustering is the most popular and dynamic research area in statistics, pattern analysis, computer vision, and it aims to cluster similar objects into the same group, and the objects fitting to different clusters are dissimilar. The minimum spanning tree

(MST) clustering process can identify the segments of arbitrary shapes by separating the consistent edges in the image. The definition of inconsistent edges is a major issue that has to be addressed in all MST-based clustering algorithms. Sometimes, the inappropriate number of image clusters, like false edges and excessive boundaries, may lead to over-segmentation[13–16]. A spanning tree is an acyclic sub-graph of a graph G, which contains all the vertices from G. The MST of a weighted graph is the minimum weight spanning tree of that graph. The cost of constructing an MST is given by, where m is the number of edges in the graph and n is the number of vertices. However, the Euclidean distance between the vertices and global as well as local densities of the vertices is defined by adjusting the variance in the Gaussian function. Correspondingly, two groups of K-cluster centers under different densities are achieved. Finally, partitioning the image clusters leads to many clusters, and the process is repeated until the optimized clusters are formed[17–20].

where, $G = (V,\ E)$ be connected, nodes and edges associated with weighted graph are given by

$$V = (v_1, v_2, v_3, \ldots\ldots, v_n\},\ \ E = \ (e_1, e_2, e_3, \ldots\ldots, e_m\}$$

Such that e_i is weighted connection among two nearer nodes $(V| = n,\ and\ \ (E| = m$

The intensity of the pixel at position (x, y) with associated node value is $v_i = I_{x,y}$. The similarity among the two nearer pixels is calculated by adding weight w_j to the edge e_j, similarly, intensity difference among the nearer pixels forms the edge e_j. The path P is a series of edges linking the two nodes in a graph G is given by

$P = \{v_i, \ldots\ldots, v_k\}$.

Correspondingly, nodes in graph G are in a form of $E' = \{v_i v_{i+1}, v_{i+1} v_{i+2}, \ldots, v_{k-1} v_k\}$

Therefore, the minimum spanning tree of a graph G, and the weight w_i connected with edge e_i of E' is,

$$T = \left(V, E^{'}\right),\ E^{'} \subseteq E\ such\ that\ \textstyle\sum_{i=1}^{m} w_i\ is\ minimum\ for\ e_i \in E^{'} \qquad (3) \qquad (3)$$

1.4 Soft threshold

A soft threshold is a pre-processing tool that estimates the optimal thresholding for sub-bands in the image. Here, image-denoising is done by either of three methods, namely Sure shrink or Bayesian shrink, or Visual shrink, based on the type of image used in the process. Appropriate filtering is employed by the machine, based on some prior knowledge and the type of the image. It provides image smoothing and better edge preservation. Since filtering is done in the wavelet domain, the detailed coefficients of the decomposed image features are processed, and pixels with intensity values above the threshold values are modified. Subsequently, the shrinkage reduces the noise without distorting the required image features[2–7], Due to the dual image filtering process, the contamination of noise details is significantly suppressed, during the image reconstruction, and at the same time, sharp image features are still retained in the wavelet restoration phase[8–10].

The sub-band dependent threshold estimation is given by

$$T_N = \frac{\beta_{\hat{\sigma}}^2}{\hat{\sigma}_y} \qquad (4) \qquad (4)$$

in every cycle,β value is calculated

$$\beta = \sqrt{log\frac{L_k}{J}} \qquad (5) \qquad (5)$$

at k^{th} cycle, L_k is the extent of sub-band, and the noise difference $\hat{\sigma}^2$ is valued by HH1 sub-band

$\hat{\sigma}^2 = [\frac{median((Y_{ij}|)}{0.6745}]^2, Y_{ij} \in subband HH1$ (6)

$\hat{\sigma}^2$ is the sub-band standard-deviation.

1.5 Statistical region merging (SRM)

The SRM algorithm belongs to the group of region merging and growing techniques combined with geometric tests to select the merging of a particular region depending on statistical criteria. In the projected study, SRM is employed by considering the segmentation errors while dealing with the clustering process. It would not be possible to separate a limited set of regions during the clustering process. Therefore, these image regions are merged by choosing the suitable decisions in computation of SRM[22–25]. The region of interest for merging image labels is based on homogeneity and similarity between the regions.

Correspondingly, merging criteria are assigned for creating native decisions, and dissimilarity measures between the pixels with the boundary of the two regions are considered. Both consistency and divergence procedures are utilized to select the merging criteria and are called statistical similarity tests [26,27].

By considering the regions R′, R of the digital image IM, if it shares the similar consistency measure, merging criteria is given by

$$P\left(R',R\right)=\begin{cases} \text{true, if } \left|{}',\bar{R}\right| \leq \sqrt{b^{2}\left(R'\right)+b^{2}\left(R\right)} \\ \text{false, otherwise} \end{cases} \tag{7}$$

where, |.| denotes the cardinality and b(R) is given by

$$b\left(R'\right)=g\sqrt{\frac{1}{2Q\left(\,R\left('\right|\right.}}ln\frac{2}{\delta} \qquad (8) \tag{8}$$

Based on the ascending order of the pixel and the difference in pixel intensities between the candidate regions considered for the merging process. The predicate is satisfied with good probability p $\geq$ 1 − N_for N merge trials,

where, (N) is the number of merging tests and maximum value of N<2 for an image IM

The numbers of regions are varied, based on image and its scaling factor [28].

This paper is organized as follows: The proposed method is discussed in section 2, and section 3 contains the flowchart of the suggested algorithm. The experimental results are given in section 4, and the conclusions are in section 5.

2 Proposed method

This paper develops a new image segmentation technique based on a machine learning platform. Here random noise is added to the standard arial image. The decomposed image is obtained from Discrete Wavelet Transform (DWT). During pre-processing stage level-2 decomposition is carried out, and approximation coefficients are subjected to a fast NL-means filter, which gives a smoothing effect while preserving edge/texture details. The usage of unsupervised learning for denoised images provides a better-segmented image. Here Minimum-Spanning Tree (MST) clustering technique is mainly used to track the complete object features, which gives more significance to full segmentation as compared to some of the popular segmentation techniques. Further Statistical Region Merging (SRM) approach extracts the required object features of the segmented image and effectively eliminates the over-segmented regions or false boundaries based on probabilistic criteria. Despite the presence of residual noise in detailed coefficients of the decomposed image is filtered automatically by the machine with the help of soft thresholding based on some prior knowledge in structural criteria of image features. Finally, the segmented image is combined with residual image details at wavelet projection, as shown in Figure 2. The resultant image is visually well understandable with meaningful and observed hidden patterns, as depicted in Figures 3, 4 and 5.

2.1 Flowchart

2.2 Algorithm steps

Input: standard Arial images are extracted from the SSIP database for analysis and segmentation.

Output: Segmented image.

· A random noise is added to the test image, and the usage of Discrete Wavelet Transform (DWT) provides the decomposed image.

· To reduce the noise, the approximation sub-image is subjected to a fast NL-means filter.

· A Minimum Spanning Tree (MST) clustering approach is assigned to partition the image details, which extract the hidden features of the image.

· The usage of Statistical Region Merging (SRM) helps to reduce the over-segmentation patterns of clustered images.

· Compatible soft threshold filter is assigned based on the structural image criteria is applied by the machine itself with its prior learning

· A combination of wavelet coefficients is displayed into full resolution at the wavelet restoration phase.

3 Results and discussions

In the proposed study, arial images are used for analysis. Here, noisy image is subjected to wavelet domain, a LL sub-image is treated with fast N-L means filter to achieve better denoising effect, and residual details are filtered automatically by considering

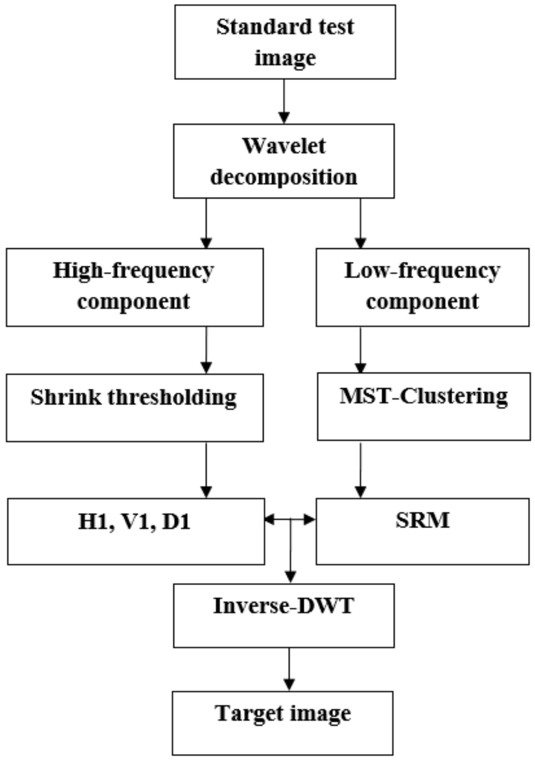

Fig 2. Functional flow diagram of the proposed method

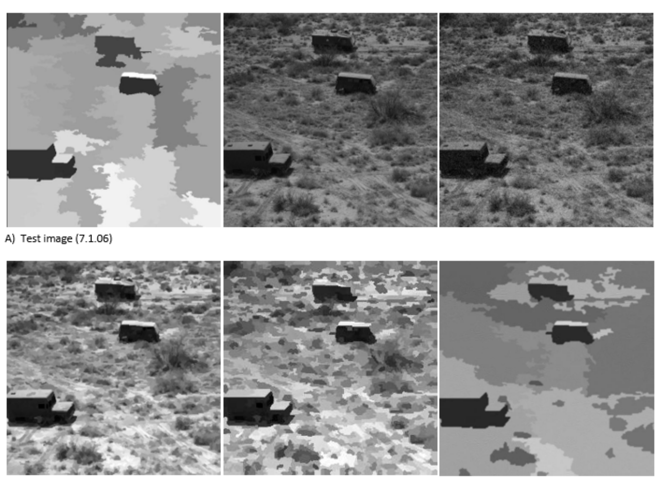

Fig 3. The performance of the denoising, segmentationand region merging with level -1, level -2, and level -3 decomposition

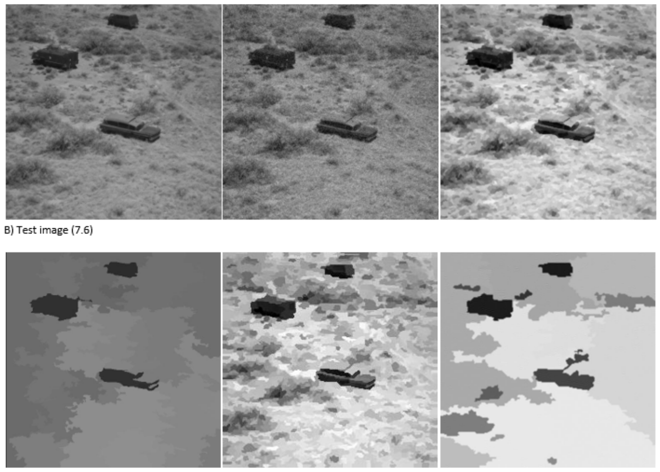

Fig 4. The performance of the denoising, segmentation and region merging with level -1, level -2, and level -3 decomposition

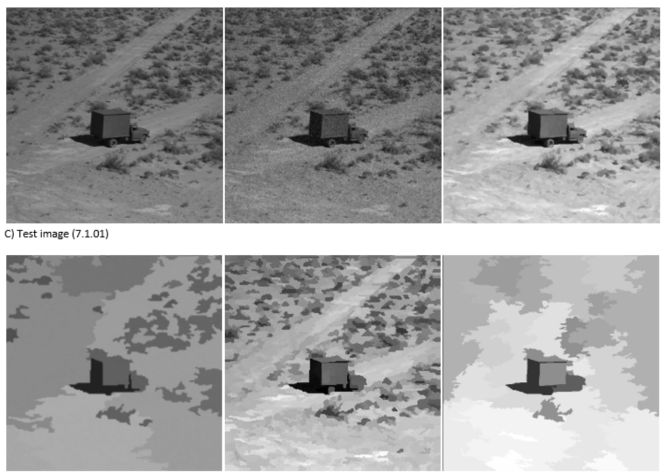

Fig 5. The performance of the denoising, segmentationand region merging with level -1, level -2, and level -3 decomposition

the structural criteria of the image based on past learning facts, hence the usage of wavelet domain filtering instead of spatial domain method is a major novelty adopted in pre-processing, before the segmentation stage. The system achieves better segmentation performance by wavelet-dependent Minimum-Spanning Tree (MST) clustering process, coupled with Statistical Region Merging (SRM) is depicted in Figures 6, 7 and 8 and segmented images help in tracking the objects in emergency conditions, and are crucial in defense applications. The simulation results are found to be better in terms of the goodness of segmentation and are illustrated in Table 1. However, 1014 segmented regions of the clustered image (7.1.06) display the robustness of segmentation, and the algorithm is efficient to track the remote objects more meaningful than other leading methods. In the merging procedure, a statistical method is used to eliminate the over-segmentation patterns to bring out 29 essential object features with residual details at level-2 decomposition is represented in Figure 3 and is one of the major novelty adopted in this work, which indicates that the system is effective while tracking the required object features in a meaningful way. Nevertheless, the usage of Discrete Curvelet Transform (DCT) preserves finer details of the image. However, the method is limited to curve and needle-shaped images, and Stationary Wavelet Transform (SWT) provides a better denoising effect due to the loss of spatial resolution and texture details. These techniques are only suitable for specific applications at the pre-processing stage. Thus DWT is utilized in the suggested algorithm, which preserves texture details and provides better spatial resolution, especially for Arial images. The PSNR values along with the time are the main criteria, in which the method excels as is evident from the results, are illustrated in Table 2, and Figure 10. The visual inspection also justifies the proposed study and provides better segmentation, especially for Arial images. Finally, the experimental results are compared with other leading methods with the combination of Hierarchical Region Merging (HRM) as well as Statistical Region Merging (SRM) techniques (Table 2, Figure 11).

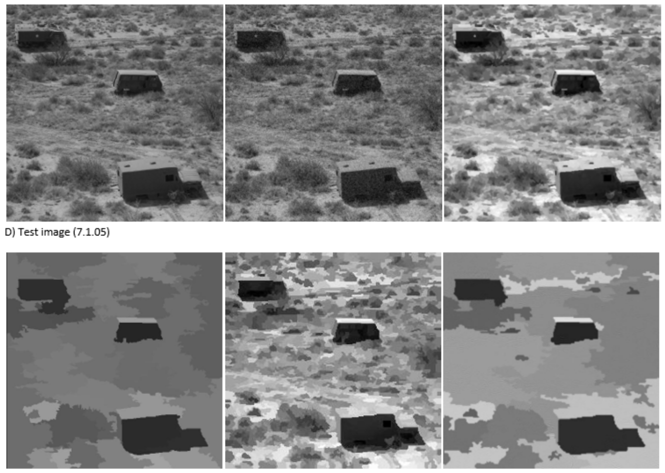

Fig 6. The performance of the denoising, segmentation and region merging with level -1,level -2, and level -3 decomposition

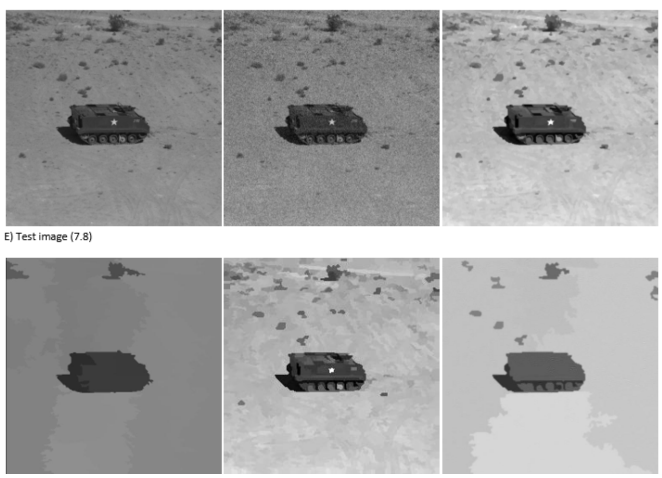

Fig 7. The performance of the denoising, segmentationand region merging with level -1, level -2, and level -3 decomposition

3.1 Performance measure

The suggested algorithm is executed in PYTHON (Spyder 3.8), and the simulation results are compared with some of the best methods available in the literature and are found to be significantly better.

3.1.1 Psnr

Peak signal to noise ratio performs the qualitative and quantitative analysis of denosing algorithms. where L is the highest pixel value and MSE gives mean square error[6–9,18,21].

$$PSNR = 10log_{10}\frac{L^2}{MSE} \qquad (9) \qquad (9)$$

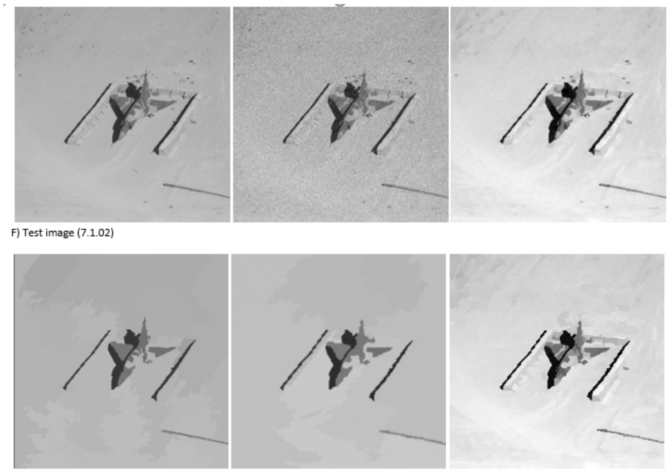

Fig 8. The performance of the denoising, segmentationand region merging with level -1, level -2, and level -3 decomposition

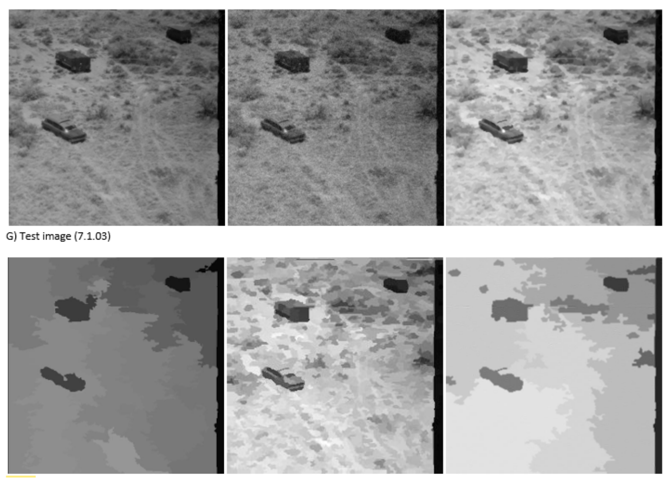

Fig 9. The performance of the denoising, segmentationand region merging with level -1, level -2, and level -3 decomposition

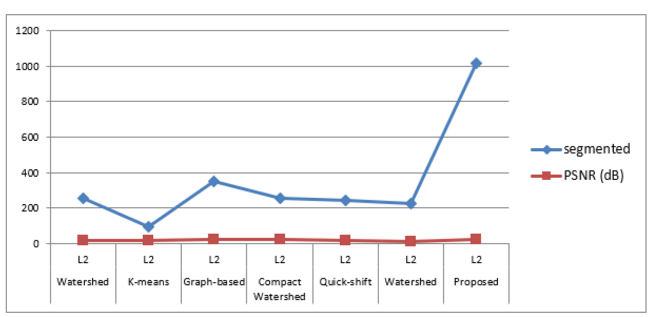

Fig 10. The comparative result of Watershed+HRM, K-means+HRM, Graph-based+HRM, Compact watershed+HRM,Quick-shift+HRM, Watershed+SRM, and Proposed method at level L-2decomposition

Table 1. The standard test image segmentation score along with PSNR values

Arial image	Decomposition Level	Estimated noise standard deviation	Segmented regions	Merged regions	PSNR (dB)	Time (s)
7.1.06	L1	0.086	3864	31	20.67	48.35
	L2	0.086	1014	29	21.72	17.96
7.6	L1	0.083	3838	23	22.67	41.45
	L2	0.082	1023	20	23.68	19.24
7.1.01	L1	0.089	3531	29	22.48	38.24
	L2	0.083	964	29	24.06	18.43
7.1.05	L1	0.086	3830	32	20.66	52.09
	L2	0.087	1052	27	21.42	35.36
7.8	L1	0.082	3593	17	25.07	66.17
	L2	0.082	990	13	26.86	50.55
7.1.02	L1	0.081	3422	24	26.83	37.51
	L2	0.081	972	15	29.01	24.89
7.1.03	L1	0.081	3827	22	22.60	43.74
	L2	0.081	1012	21	23.93	23.39

Table 2. The performance of the existing segmentation methods with proposed study

Arial image 7.1.06	**Watershed+HRM**	**K-means+HRM**	**Graph-based+HRM**	**Compact Watershed+HRM**	**Quick-shift+HRM**	**Watershed+SRM**	**Proposed method**
Level	2	2	2	2	2	2	2
Segmented	254	94	350	256	244	225	1014
Merged	120	163	191	174	166	16	29
PSNR (dB)	16.89	20	21.70	21.41	15.11	14.07	21.73
Time(s)	41.75	26.64	22.92	20.96	71.13	16.59	17.96

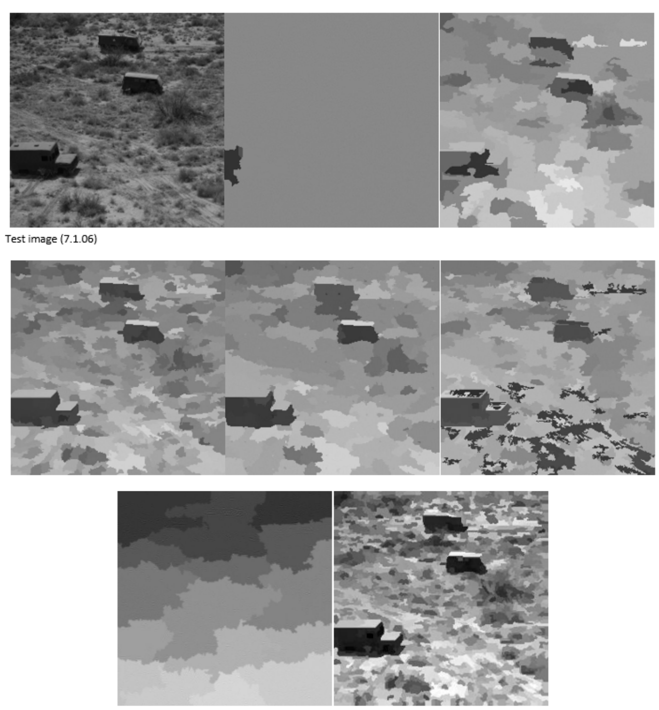

Fig 11. The comparative outcome of Watershed+HRM, K-means+HRM, Graph-based+HRM, Compact watershed+HRM,Quick-shift+HRM Watershed+SRM, and Proposed study at level L-2decomposition

4 Conclusion

In this paper, a machine learning-based image clustering technique is developed using wavelet transform. During the pre-processing stage, approximation image coefficients are denoised by a fast NL-means filter which provides a better denoising effect on random noise compared to other leading methods. A suitable soft thresholding value is automatically selected based on structural criteria of the high-frequency image details is one of the key steps in the proposed algorithm. Here SRM help in eliminating the false boundaries of segmented images and in overcoming the drawbacks of clustering algorithm by reducing the over-segmentation patterns to enhance the necessary hidden image details. Finally, both image features are fused at the wavelet projection level. However, in existing methods especially in arial image analysis, the segmented outcome is not possible to meet the desired level, due to an under-segmentation process. Thus the post-processing stage produces only a few image features while merging in level-2 decomposition. Therefore, the article suggests a new method for standard and Arial image analysis. In the segmentation process, the usage of the clustering technique efficiently segments the crucial details of the denoised image (7.1.06) and significantly overcomes the under-segmentation issues. Therefore the algorithm is more effective in detecting the image patterns as compared to some of the leading segmentation techniques and is one of the major novelty implemented in this work, which helps in the merging process to acquire essential and meaningful features of the segmented image, as shown in Figure 7, 8, and 9. However, the watershed-based hierarchical region merging (HRM) method provides 254 segments and 120 regions, and a graph-based hierarchical region merging approach achieved 350 segments and 94 regions, which were better than K-means + HRM, compact watershed + HRM, and quick shift + HRM models. The proposed SRM dependent clustering algorithm achieved 1014 segments and 29 essential object features with residual features is shown in Figure 11. Hence the suggested model is more efficient in extracting the vital details of the arial image and recognizing the object features at the wavelet restoration level. The projected image provides a 21.73 PSNR value in 17.96 elapsed time, and is compared with some of the popular segmentation techniques along with time are illustrated in Figure 11, and Table 2. Also, the visual evaluation justifies the suggested study is better than the existing methods. The utilization of wavelet transform to preserve edge features during segmentation is one of the key features of this method, and it significantly overcomes the under segmentation patterns. The entire proposed system works better in segmenting both general and arial images and it is a key advantage in various applications. Also, object features of the arial image are well recognized by the segmented image and are critical in warfare conditions is another key contribution of this technique.

References

1) Yin S, Zhang Y, Karim S. Large Scale Remote Sensing Image Segmentation Based on Fuzzy Region Competition and Gaussian Mixture Model. *IEEE Access*. 2018;6:26069–26080. Available from: https://dx.doi.org/10.1109/access.2018.2834960.
2) Li X, Li T, Wang Y. GW-DC: A Deep Clustering Model Leveraging Two-Dimensional Image Transformation and Enhancement. *Algorithms*. 2021;14(12):349–349. Available from: https://dx.doi.org/10.3390/a14120349.
3) Lv X, Ma Y, He X, Huang H, Yang J. CciMST: A Clustering Algorithm Based on Minimum Spanning Tree and Cluster Centers. *Mathematical Problems in Engineering*. 2018;2018:1–14. Available from: https://dx.doi.org/10.1155/2018/8451796.
4) Wang M, Dong Z, Cheng Y, Li D. Optimal Segmentation of High-Resolution Remote Sensing Image by Combining Superpixels With the Minimum Spanning Tree. *IEEE Transactions on Geoscience and Remote Sensing*. 2018;56(1):228–238. Available from: https://dx.doi.org/10.1109/tgrs.2017.2745507.
5) Rani P, Kotwal S, Manhas J. Machine learning and deep learning based computational approaches in automatic microorganisms image recognition: methodologies, challenges, and developments. *Archives of Computational Methods in Engineering*. 2021. Available from: https://doi.org/10.1007/s11831-021.
6) Wang Z. Unsupervised Wavelet-Feature Markov Clustering Algorithm for Remotely Sensed Images. *2020 IEEE International Symposium on Signal Processing and Information Technology (ISSPIT)*. 2021. doi:10.1109/ISSPIT51521.2020.9408754.
7) Verma AK, Vamsi I, Saurabh P, Sudha R, Sabareesh GR, Rajkumar S. Wavelet and deep learning-based detection of SARS-nCoV from thoracic X-ray images for rapid and efficient testing. *Expert Systems with Applications*. 2021;185:115650–115650. Available from: https://dx.doi.org/10.1016/j.eswa.2021.115650.
8) Tania M, Afroze D, Akhter J, Sayed MA, Rahaman M, Islam MI. Image recognition using machine learning with the aid of MLR. *Image Graphics and Signal Processing*. 2021;6:12–22. doi:10.5815/ijigsp.2021.06.02.
9) Arumugadevi S, Seenivasagam V. Comparison of Clustering Methods for Segmenting Color Images. *Indian Journal of Science and Technology*. 2015;8(7):670–670. Available from: https://dx.doi.org/10.17485/ijst/2015/v8i7/62862.
10) Jena S, Mohanty MD, Mohanty MN. Biomedical Image Segmentation using Optimized Fuzzy C-mean Algorithm. *Indian Journal of Science and Technology*. 2017;10(35):1–6.
11) Amin J, Sharif M, Haldorai A, Yasmin M, Nayak RS. Brain tumor detection and classification using machine learning: a comprehensive survey. *Complex & Intelligent Systems*. 2021;p. 1–23. Available from: https://dx.doi.org/10.1007/s40747-021-00563-y.
12) jaina L, Singh BP. A novel wavelet thresholding rule for speckle reduction from ultrasound images . *Journal of King Saud University - Computer and Information Sciences*. 2020. Available from: https://doi.org/10.1016/j.jksuci.2020.10.009.
13) Felzenszwalb PF, Huttenlocher DP. Efficient Graph-Based Image Segmentation. *International Journal of Computer Vision*. 2004;59(2):167–181. Available from: https://dx.doi.org/10.1023/b:visi.0000022288.19776.77.
14) Huchan JJ, Jiang BO. Wavelet transform and morphology image segmentation algorism for blood cell. *Industrial Electronics and Applications (ICIEA)*. 2009;978(1). doi:10.1109/ICIEA.2009.5138265.

15) Raj A, Radhakrishnan AK, B. A comparative study on target detection in military field using various digital image processing techniques. *International Journal of Computer Science and Network (IJCSN)*. 2016;5(1):2277–5420.
16) Dhanachandra N, Chanu YJ. A new image segmentation method using clustering and region merging techniques. *Advances in Intelligent Systems and Computing, Applications of Artificial Intelligence Techniques in Engineering*. 2019;p. 603–614. doi:10.1007/978-981-13-1819-1_57.
17) Nija KS, Anupama CP, Gopi VP, Anitha VS. Automated segmentation of optic disc using statistical region merging and morphological operations. *Physical and Engineering Sciences in Medicine*. 2020;43(3):857–869. Available from: https://dx.doi.org/10.1007/s13246-020-00883-2.
18) Li Z, Zhang W, Yang H. Color Image Segmentation Based on Wavelet Transform and Fuzzy Kernel Clustering. *International Conference on Virtual Reality and Intelligent Systems (ICVRIS)*. 2020;2020:411–414. doi:10.1109/ICVRIS51417.2020.00103.
19) Ijitona TB, Ren J, Hwang PB. SAR sea ice image segmentation using watershed with intensity-based region merging. *Computer and Information Technology IEEE*. 2014;6(14):978–979. doi:10.1109/CIT.2014.19.
20) Mukhopadhyay J, Choudhuri S, Sengupta S. ANFIS based speed and current control with torque ripple minimization using hybrid SSD-SFO for switched reluctance motor. *Sustainable Energy Technologies and Assessments*. 2022;49:101712–101712. Available from: https://dx.doi.org/10.1016/j.seta.2021.101712.
21) Pun CM, An NY, Chen CLP. Region-based Image Segmentation by Watershed Partition and DCT Energy Compaction. *International Journal of Computational Intelligence Systems*. 2012;5(1):53–53. Available from: https://dx.doi.org/10.1080/18756891.2012.670521.
22) Angelina S, Suresh LP, Veni SHK. Image segmentation based on genetic algorithm for region growth and region merging. *International Conference on Computing, Electronics and Electrical Technologies (ICCEET)*. 2012. doi:10.1109/ICCEET.2012.6203833.
23) Peng B, Zhang L, Zhang D. Automatic Image Segmentation by Dynamic Region Merging. *IEEE Transactions on Image Processing*. 2011;20(12):3592–3605. Available from: https://dx.doi.org/10.1109/tip.2011.2157512.
24) Ko BC, Gim JW, Nam JY. Automatic white blood cell segmentation using stepwise merging rules and gradient vector flow snake. *Micron*. 2011;42:695–705. Available from: https://dx.doi.org/10.1016/j.micron.2011.03.009.
25) Pun CM, An NY. Image segmentation using effective region merging strategy. *International Journal of Digital Technology and its Application*. 2011;5(8):59–69. doi:10.4156/jdcta.vol5.issue8.8.
26) Basavaprasad B, Hegadi RS. Automatic multi stage image segmentation using normalized cut in gradient image. *Advances in Computational Sciences and Technology*. 2017;10(1):37–51.
27) Wang Y, Meng Q, Qi Q, Yang J, Liu Y. Region Merging Considering Within- and Between-Segment Heterogeneity: An Improved Hybrid Remote-Sensing Image Segmentation Method. *Remote Sensing*. 2018;10(5):781–781. Available from: https://dx.doi.org/10.3390/rs10050781.
28) Pitchai R, Supraja P, Victoria AH, Madhavi M. Brain Tumor Segmentation Using Deep Learning and Fuzzy K-Means Clustering for Magnetic Resonance Images. *Neural Processing Letters*. 2021;53(4):2519–2532. Available from: https://dx.doi.org/10.1007/s11063-020-10326-4.